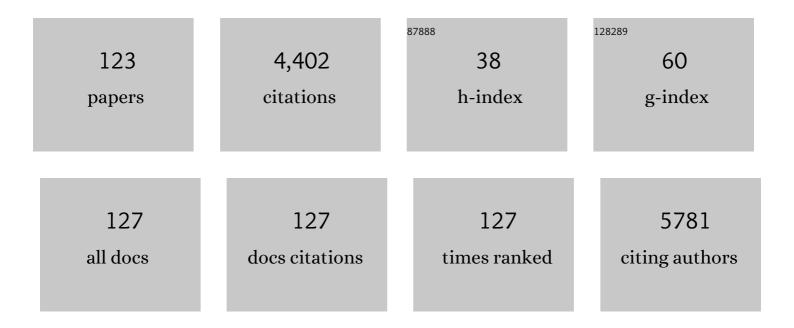
List of Publications by Year in descending order

Source: https://exaly.com/author-pdf/7837673/publications.pdf Version: 2024-02-01



ΟΙΙΙΗΙΟΡΑσην

#	Article	IF	CITATIONS
1	Metabolism of hyperpolarised [1– ¹³ C]pyruvate in awake and anaesthetised rat brains. NMR in Biomedicine, 2022, 35, e4635.	2.8	7
2	Infantile status epilepticus disrupts myelin development. Neurobiology of Disease, 2022, 162, 105566.	4.4	3
3	Eventâ€recurring multiband SWIFT functional MRI with 200â€ms temporal resolution during deep brain stimulation and isofluraneâ€induced burst suppression in rat. Magnetic Resonance in Medicine, 2022, , .	3.0	0
4	Light sedation with short habituation time for largeâ€scale functional magnetic resonance imaging studies in rats. NMR in Biomedicine, 2022, 35, e4679.	2.8	3
5	Whole-brain studies of spontaneous behavior in head-fixed rats enabled by zero echo time MB-SWIFT fMRI. NeuroImage, 2022, 250, 118924.	4.2	3
6	Chronic hypometabolism in striatum and hippocampal network after traumatic brain injury and their relation with memory impairment – [18F]-FDG-PET and MRI 4Âmonths after fluid percussion injury in rat. Brain Research, 2022, 1788, 147934.	2.2	5
7	Orientation selective DBS of entorhinal cortex and medial septal nucleus modulates activity of rat brain areas involved in memory and cognition. Scientific Reports, 2022, 12, .	3.3	0
8	Quantitative susceptibility mapping of the rat brain after traumatic brain injury. NMR in Biomedicine, 2021, 34, e4438.	2.8	20
9	Assessment of the structural complexity of diffusion MRI voxels using 3D electron microscopy in the rat brain. Neurolmage, 2021, 225, 117529.	4.2	8
10	Data-Driven Regularization Parameter Selection in Dynamic MRI. Journal of Imaging, 2021, 7, 38.	3.0	1
11	Brain fMRI during orientation selective epidural spinal cord stimulation. Scientific Reports, 2021, 11, 5504.	3.3	2
12	Automated joint skull-stripping and segmentation with Multi-Task U-Net in large mouse brain MRI databases. NeuroImage, 2021, 229, 117734.	4.2	22
13	Spinal cord fMRI with MBâ€5WIFT for assessing epidural spinal cord stimulation in rats. Magnetic Resonance in Medicine, 2021, 86, 2137-2145.	3.0	5
14	lsoflurane affects brain functional connectivity in rats 1 month after exposure. Neurolmage, 2021, 234, 117987.	4.2	18
15	Acute thalamic damage as a prognostic biomarker for postâ€ŧraumatic epileptogenesis. Epilepsia, 2021, 62, 1852-1864.	5.1	14
16	Ratiometric magnetic resonance imaging: Contrast agent design towards better specificity and quantification. Coordination Chemistry Reviews, 2021, 447, 214150.	18.8	14
17	Steerable3D: An ImageJ plugin for neurovascular enhancement in 3-D segmentation. Physica Medica, 2021, 81, 197-209.	0.7	5
18	Microstructural Tissue Changes in a Rat Model of Mild Traumatic Brain Injury. Frontiers in Neuroscience, 2021, 15, 746214.	2.8	6

#	Article	IF	CITATIONS
19	Detection of lentiviral suicide gene therapy in C6 rat glioma using hyperpolarised [1―13 C]pyruvate. NMR in Biomedicine, 2020, 33, e4250.	2.8	3
20	Multi-band SWIFT enables quiet and artefact-free EEG-fMRI and awake fMRI studies in rat. NeuroImage, 2020, 206, 116338.	4.2	23
21	Temporal Huber Regularization for DCE-MRI. Journal of Mathematical Imaging and Vision, 2020, 62, 1334-1346.	1.3	4
22	Long-lasting blood-brain barrier dysfunction and neuroinflammation after traumatic brain injury. Neurobiology of Disease, 2020, 145, 105080.	4.4	92
23	Early Increase in Cortical T ₂ Relaxation Is a Prognostic Biomarker for the Evolution of Severe Cortical Damage, but Not for Epileptogenesis, after Experimental Traumatic Brain Injury. Journal of Neurotrauma, 2020, 37, 2580-2594.	3.4	15
24	Orientation selective deep brain stimulation of the subthalamic nucleus in rats. NeuroImage, 2020, 213, 116750.	4.2	7
25	MRS Reveals Chronic Inflammation in T2w MRI-Negative Perilesional Cortex – A 6-Months Multimodal Imaging Follow-Up Study. Frontiers in Neuroscience, 2019, 13, 863.	2.8	13
26	Determining T2 relaxation time and stroke onset relationship in ischaemic stroke within apparent diffusion coefficient-defined lesions. A user-independent method for quantifying the impact of stroke in the human brain. Biomedical Spectroscopy and Imaging, 2019, 8, 11-28.	1.2	4
27	Mechanosensitive meningeal nociception via Piezo channels: Implications for pulsatile pain in migraine?. Neuropharmacology, 2019, 149, 113-123.	4.1	57
28	Harmonization of pipeline for preclinical multicenter MRI biomarker discovery in a rat model of post-traumatic epileptogenesis. Epilepsy Research, 2019, 150, 46-57.	1.6	25
29	Imaging biomarkers of epileptogenecity after traumatic brain injury – Preclinical frontiers. Neurobiology of Disease, 2019, 123, 75-85.	4.4	23
30	Sleep-State Dependent Alterations in Brain Functional Connectivity under Urethane Anesthesia in a Rat Model of Early-Stage Parkinson's Disease. ENeuro, 2019, 6, ENEURO.0456-18.2019.	1.9	9
31	Functional connectivity under six anesthesia protocols and the awake condition in rat brain. NeuroImage, 2018, 172, 9-20.	4.2	217
32	Quantification of anisotropy and orientation in 3D electron microscopy and diffusion tensor imaging in injured rat brain. NeuroImage, 2018, 172, 404-414.	4.2	36
33	Nucleiâ€specific deposits of iron and calcium in the rat thalamus after status epilepticus revealed with quantitative susceptibility mapping (QSM). Journal of Magnetic Resonance Imaging, 2018, 47, 554-564.	3.4	26
34	State Estimation with Structural Priors in fMRI. Journal of Mathematical Imaging and Vision, 2018, 60, 174-188.	1.3	5
35	Tuning Neuromodulation Effects by Orientation Selective Deep Brain Stimulation in the Rat Medial Frontal Cortex. Frontiers in Neuroscience, 2018, 12, 899.	2.8	9
36	Awake Rat Brain Functional Magnetic Resonance Imaging Using Standard Radio Frequency Coils and a 3D Printed Restraint Kit. Frontiers in Neuroscience, 2018, 12, 548.	2.8	55

#	Article	IF	CITATIONS
37	Dynamic MRI reconstruction from undersampled data with an anatomical prescan. Inverse Problems, 2018, 34, 074001.	2.0	16
38	Common data elements and data management: Remedy to cure underpowered preclinical studies. Epilepsy Research, 2017, 129, 87-90.	1.6	35
39	Magnetization transfer SWIFT MRI consistently detects histologically verified myelin loss in the thalamocortical pathway after a traumatic brain injury in rat. NMR in Biomedicine, 2017, 30, e3678.	2.8	24
40	Diffusion tensor MRI shows progressive changes in the hippocampus and dentate gyrus after status epilepticus in rat – histological validation with Fourier-based analysis. NeuroImage, 2017, 152, 221-236.	4.2	40
41	Dose-response effect of acute phencyclidine on functional connectivity and dopamine levels, and their association with schizophrenia-like symptom classes in rat. Neuropharmacology, 2017, 119, 15-25.	4.1	13
42	Orientation selective deep brain stimulation. Journal of Neural Engineering, 2017, 14, 016016.	3.5	41
43	MB-SWIFT functional MRI during deep brain stimulation in rats. NeuroImage, 2017, 159, 443-448.	4.2	25
44	Neuroimaging in animal models of epilepsy. Neuroscience, 2017, 358, 277-299.	2.3	18
45	Restingâ€state functional MRI as a tool for evaluating brain hemodynamic responsiveness to external stimuli in rats. Magnetic Resonance in Medicine, 2017, 78, 1136-1146.	3.0	16
46	In Vivo Imaging in Rodents. , 2017, , 197-215.		0
47	Stroke onset time determination using MRI relaxation times without non-ischaemic reference in a rat stroke model. Biomedical Spectroscopy and Imaging, 2017, 6, 25-35.	1.2	10
48	Searching for epilepsy's crystal ball. ELife, 2017, 6, .	6.0	0
49	Global Functional Connectivity Differences between Sleep-Like States in Urethane Anesthetized Rats Measured by fMRI. PLoS ONE, 2016, 11, e0155343.	2.5	24
50	Stroke onset time estimation from multispectral quantitative magnetic resonance imaging in a rat model of focal permanent cerebral ischemia. International Journal of Stroke, 2016, 11, 677-682.	5.9	11
51	Protective Effects and Magnetic Resonance Imaging Temperature Mapping of Systemic and Focal Hypothermia in Cerebral Ischemia. Stroke, 2016, 47, 2386-2396.	2.0	21
52	MRI relaxation in the presence of fictitious fields correlates with myelin content in normal rat brain. Magnetic Resonance in Medicine, 2016, 75, 161-168.	3.0	33
53	Tailored Dual PEGylation of Inorganic Porous Nanocarriers for Extremely Long Blood Circulation in Vivo. ACS Applied Materials & Interfaces, 2016, 8, 32723-32731.	8.0	39
54	Implantable RF-coil with multiple electrodes for long-term EEG-fMRI monitoring in rodents. Journal of Neuroscience Methods, 2016, 274, 154-163.	2.5	15

#	Article	IF	CITATIONS
55	Advances in the development of biomarkers for epilepsy. Lancet Neurology, The, 2016, 15, 843-856.	10.2	283
56	Effect of collagen cross-linking on quantitative MRI parameters of articular cartilage. Osteoarthritis and Cartilage, 2016, 24, 1656-1664.	1.3	5
57	A spatiotemporal theory for MRI T2 relaxation time and apparent diffusion coefficient in the brain during acute ischaemia: Application and validation in a rat acute stroke model. Journal of Cerebral Blood Flow and Metabolism, 2016, 36, 1232-1243.	4.3	9
58	Comparison of seven different anesthesia protocols for nicotine pharmacologic magnetic resonance imaging in rat. European Neuropsychopharmacology, 2016, 26, 518-531.	0.7	52
59	Early Maternal Alcohol Consumption Alters Hippocampal DNA Methylation, Gene Expression and Volume in a Mouse Model. PLoS ONE, 2015, 10, e0124931.	2.5	63
60	Brain Amyloidosis and BDNF Deficiency Have Opposite Effects on Brain Volumes in AβPP/PS1 Mice Both in vivo and ex vivo. Journal of Alzheimer's Disease, 2015, 46, 929-946.	2.6	6
61	Involvement of NMDA receptor subtypes in cortical spreading depression in rats assessed by fMRI. Neuropharmacology, 2015, 93, 164-170.	4.1	39
62	Phase imaging in brain using SWIFT. Journal of Magnetic Resonance, 2015, 252, 20-28.	2.1	4
63	Measurement of T ₁ relaxation time of osteochondral specimens using VFAâ€SWIFT. Magnetic Resonance in Medicine, 2015, 74, 175-184.	3.0	15
64	Diffusion tensor imaging of hippocampal network plasticity. Brain Structure and Function, 2015, 220, 781-801.	2.3	51
65	Progressive Volume Loss and White Matter Degeneration in Cstb-Deficient Mice: A Diffusion Tensor and Longitudinal Volumetry MRI Study. PLoS ONE, 2014, 9, e90709.	2.5	19
66	Decreased Resting Functional Connectivity after Traumatic Brain Injury in the Rat. PLoS ONE, 2014, 9, e95280.	2.5	54
67	Timing the ischaemic stroke by 1H-MRI. NeuroReport, 2014, 25, 1180-1185.	1.2	13
68	Posttraumatic epilepsy $\hat{a} \in $ Disease or comorbidity?. Epilepsy and Behavior, 2014, 38, 19-24.	1.7	41
69	Facile synthesis of biocompatible superparamagnetic mesoporous nanoparticles for imageable drug delivery. Microporous and Mesoporous Materials, 2014, 195, 2-8.	4.4	15
70	Opposite Reactivity of Meningeal versus Cortical Microvessels to the Nitric Oxide Donor Glyceryl Trinitrate Evaluated In Vivo with Two-Photon Imaging. PLoS ONE, 2014, 9, e89699.	2.5	8
71	Longitudinal rotating frame relaxation time measurements in infarcted mouse myocardium in vivo. Magnetic Resonance in Medicine, 2013, 69, 1389-1395.	3.0	35
72	MRI Biomarkers for Post-Traumatic Epileptogenesis. Journal of Neurotrauma, 2013, 30, 1305-1309.	3.4	53

#	Article	lF	CITATIONS
73	White Matter Degeneration with Unverricht-Lundborg Progressive Myoclonus Epilepsy: A Translational Diffusion-Tensor Imaging Study in Patients and Cystatin B–Deficient Mice. Radiology, 2013, 269, 232-239.	7.3	40
74	Relaxation Along a Fictitious Field (RAFF) and Z-spectroscopy using Alternating-Phase Irradiation (ZAPI) in Permanent Focal Cerebral Ischemia in Rat. PLoS ONE, 2013, 8, e69157.	2.5	4
75	Detection of calcifications in vivo and ex vivo after brain injury in rat using SWIFT. NeuroImage, 2012, 61, 761-772.	4.2	39
76	Glioma cell density in a rat gene therapy model gauged by water relaxation rate along a fictitious magnetic field. Magnetic Resonance in Medicine, 2012, 67, 269-277.	3.0	21
77	Rats Bred for Low Aerobic Capacity Become Promptly Fatigued and Have Slow Metabolic Recovery after Stimulated, Maximal Muscle Contractions. PLoS ONE, 2012, 7, e48345.	2.5	9
78	Multimodal MRI assessment of damage and plasticity caused by status epilepticus in the rat brain. Epilepsia, 2011, 52, 57-60.	5.1	21
79	Chronic Hyperperfusion and Angiogenesis Follow Subacute Hypoperfusion in the Thalamus of Rats with Focal Cerebral Ischemia. Journal of Cerebral Blood Flow and Metabolism, 2011, 31, 1119-1132.	4.3	33
80	Magnetic Resonance Imaging of Regional Hemodynamic and Cerebrovascular Recovery after Lateral Fluid-Percussion Brain Injury in Rats. Journal of Cerebral Blood Flow and Metabolism, 2011, 31, 166-177.	4.3	64
81	Diffusion tensor MRI with tract-based spatial statistics and histology reveals undiscovered lesioned areas in kainate model of epilepsy in rat. Brain Structure and Function, 2011, 216, 123-135.	2.3	50
82	Evoked local field potentials can explain temporal variation in blood oxygenation levelâ€dependent responses in rat somatosensory cortex. NMR in Biomedicine, 2011, 24, 209-215.	2.8	6
83	Estimation of the Onset Time of Cerebral Ischemia Using T _{1ï} and T ₂ MRI in Rats. Stroke, 2010, 41, 2335-2340.	2.0	55
84	Simultaneous fMRI and local field potential measurements during epileptic seizures in medetomidineâ€sedated rats using raser pulse sequence. Magnetic Resonance in Medicine, 2010, 64, 1191-1199.	3.0	38
85	Correlating Tissue Outcome with Quantitative Multiparametric MRI of Acute Cerebral Ischemia in Rats. Journal of Cerebral Blood Flow and Metabolism, 2010, 30, 415-427.	4.3	32
86	Cerebral Blood Volume Alterations in the Perilesional Areas in the Rat Brain after Traumatic Brain Injury—Comparison with Behavioral Outcome. Journal of Cerebral Blood Flow and Metabolism, 2010, 30, 1318-1328.	4.3	30
87	Association of Chronic Vascular Changes with Functional Outcome after Traumatic Brain Injury in Rats. Journal of Neurotrauma, 2010, 27, 2203-2219.	3.4	76
88	Diffusion tensor MRI of axonal plasticity in the rat hippocampus. NeuroImage, 2010, 51, 521-530.	4.2	69
89	Elevated cerebral blood flow and vascular density in the amygdala after status epilepticus in rats. Neuroscience Letters, 2010, 484, 39-42.	2.1	17
90	Distinct MRI pattern in lesional and perilesional area after traumatic brain injury in rat — 11Âmonths follow-up. Experimental Neurology, 2009, 215, 29-40.	4.1	72

#	Article	IF	CITATIONS
91	Quantitative MRI predicts long-term structural and functional outcome after experimental traumatic brain injury. NeuroImage, 2009, 45, 1-9.	4.2	97
92	A multi-metabolite analysis of serum by 1H NMR spectroscopy: Early systemic signs of Alzheimer's disease. Biochemical and Biophysical Research Communications, 2008, 375, 356-361.	2.1	104
93	Coupling between simultaneously recorded BOLD response and neuronal activity in the rat somatosensory cortex. NeuroImage, 2008, 39, 775-785.	4.2	117
94	Manganese enhanced MRI detects mossy fiber sprouting rather than neurodegeneration, gliosis or seizure-activity in the epileptic rat hippocampus. NeuroImage, 2008, 40, 1718-1730.	4.2	53
95	Quantitative diffusion MRI of hippocampus as a surrogate marker for post-traumatic epileptogenesis. Brain, 2007, 130, 3155-3168.	7.6	129
96	Adenovirus-Mediated Gene Transfer of Human Vascular Endothelial Growth Factor-D Induces Transient Angiogenic Effects in Mouse Hind Limb Muscle. Human Gene Therapy, 2007, 18, 232-244.	2.7	23
97	Non-invasive Imaging in Gene Therapy. Molecular Therapy, 2007, 15, 1579-1586.	8.2	52
98	Subacute hemorrhage and resolution of edema in Rose Bengal stroke model in rats coincides with improved sensorimotor functions. Neuroscience Letters, 2007, 428, 99-102.	2.1	17
99	Therapeutic angiogenesis induced by gene transfer of placental growth factor improves exercise tolerance of ischemic rabbit hindlimbs. International Journal of Cardiology, 2007, 119, S1-S2.	1.7	Ο
100	High resolution ultrasound perfusion imaging of therapeutic angiogenesis. International Journal of Cardiology, 2007, 119, S8.	1.7	0
101	Manganese-enhanced magnetic resonance imaging of mossy fiber plasticity in vivo. NeuroImage, 2006, 30, 130-135.	4.2	53
102	Antioxidant pyrrolidine dithiocarbamate activates Akt–GSK signaling and is neuroprotective in neonatal hypoxia–ischemia. Free Radical Biology and Medicine, 2006, 40, 1776-1784.	2.9	49
103	Experimental Febrile Seizures Require an Undetermined Factor for Induction of Hippocampal Sclerosis in Immature Rat Brain. Epilepsy Currents, 2005, 5, 98-100.	0.8	1
104	Tumour Gene Therapy Monitoring Using Magnetic Resonance Imaging and Spectroscopy. Current Gene Therapy, 2005, 5, 685-696.	2.0	11
105	Progression of Brain Damage after Status Epilepticus and Its Association with Epileptogenesis: A Quantitative MRI Study in a Rat Model of Temporal Lobe Epilepsy. Epilepsia, 2004, 45, 1024-1034.	5.1	132
106	Metabolite Changes in BT4C Rat Gliomas Undergoing Ganciclovir-Thymidine Kinase Gene Therapy-induced Programmed Cell Death as Studied by 1H NMR Spectroscopy in Vivo, ex Vivo, and in Vitro. Journal of Biological Chemistry, 2003, 278, 45915-45923.	3.4	66
107	Assignment of 1H nuclear magnetic resonance visible polyunsaturated fatty acids in BT4C gliomas undergoing ganciclovir-thymidine kinase gene therapy-induced programmed cell death. Cancer Research, 2003, 63, 3195-201.	0.9	111
108	Novel magnetic resonance imaging contrasts for monitoring response to gene therapy in rat glioma. Cancer Research, 2003, 63, 7571-4.	0.9	25

#	Article	IF	CITATIONS
109	Progression of neuronal damage after status epilepticus and during spontaneous seizures in a rat model of temporal lobe epilepsy. Progress in Brain Research, 2002, 135, 67-83.	1.4	182
110	Early gene therapy–induced apoptotic response in BT4C gliomas by magnetic resonance relaxation contrast T1 in the rotating frame. Cancer Gene Therapy, 2002, 9, 338-345.	4.6	56
111	Quantitative Assessment of the Balance between Oxygen Delivery and Consumption in the Rat Brain after Transient Ischemia with T2-BOLD Magnetic Resonance Imaging. Journal of Cerebral Blood Flow and Metabolism, 2002, 22, 262-270.	4.3	27
112	Quantitative T1ϕand Magnetization Transfer Magnetic Resonance Imaging of Acute Cerebral Ischemia in the Rat. Journal of Cerebral Blood Flow and Metabolism, 2002, 22, 547-558.	4.3	40
113	Proton Exchange as a Relaxation Mechanism for T1 in the Rotating Frame in Native and Immobilized Protein Solutions. Biochemical and Biophysical Research Communications, 2001, 289, 813-818.	2.1	84
114	Graded Reduction of Cerebral Blood Flow in Rat as Detected by the Nuclear Magnetic Resonance Relaxation Time T ₂ : A Theoretical and Experimental Approach. Journal of Cerebral Blood Flow and Metabolism, 2000, 20, 316-326.	4.3	54
115	Early Detection of Irreversible Cerebral Ischemia in the Rat Using Dispersion of the Magnetic Resonance Imaging Relaxation Time, T1ï• Journal of Cerebral Blood Flow and Metabolism, 2000, 20, 1457-1466.	4.3	95
116	Transgenic Mice Overexpressing Truncated trkB Neurotrophin Receptors in Neurons Show Increased Susceptibility to Cortical Injury after Focal Cerebral Ischemia. Molecular and Cellular Neurosciences, 2000, 16, 87-96.	2.2	79
117	Enhanced ornithine decarboxylase activity is associated with attenuated rate of damage evolution and reduction of infarct volume in transient middle cerebral artery occlusion in the rat1Published on the World Wide Web on 17 March 1999.1. Brain Research, 1999, 826, 325-329.	2.2	14
118	Noninvasive Detection of Cerebral Hypoperfusion and Reversible Ischemia from Reductions in the Magnetic Resonance Imaging Relaxation Time, T2. Journal of Cerebral Blood Flow and Metabolism, 1998, 18, 911-920.	4.3	83
119	Neuroprotective role of ornithine decarboxylase activation in transient focal cerebral ischaemia: a study using ornithine decarboxylase-overexpressing transgenic rats. European Journal of Neuroscience, 1998, 10, 2046-2055.	2.6	33
120	Increased macromolecular resonances in the rat cerebral cortex during severe energy failure as detected by 1H nuclear magnetic resonance spectroscopy. Neuroscience Letters, 1996, 212, 151-154.	2.1	16
121	Intracellular chelation of calcium prevents cell damage following severe hypoxia in the rat cerebral cortex as studied by NMR spectroscopy ex vivo. Cell Calcium, 1996, 20, 509-514.	2.4	4
122	State Estimation of Time-Varying MRI with Radial Golden Angle Sampling. Journal of Mathematical Imaging and Vision, 0, , .	1.3	0
123	Spatial signatures of anesthesia-induced burst-suppression differ between primates and rodents. ELife, 0, 11, .	6.0	8